UDC 621.3 https://doi.org/10.20998/2074-272X.2023.4.03

A. Khemis, T. Boutabba, S. Drid

Model reference adaptive system speed estimator based on type-1 and type-2 fuzzy logic sensorless control of electrical vehicle with electrical differential

Introduction. *In this paper, a new approach for estimating the speed of in-wheel electric vehicles with two independent rear drives is presented. Currently, the variable-speed induction motor replaces the DC motor drive in a wide range of applications, including electric vehicles where quick dynamic response is required. This is now possible as a result of significant improvements in the dynamic performance of electrical drives brought about by technological advancements and development in the fields of power commutation devices, digital signal processing, and, more recently, intelligent control systems. The system's reliability and robustness are improved, and the cost, size, and upkeep requirements of the induction motor drive are reduced through control strategies without a speed sensor. Successful uses of the induction motor without a sensor have been made for medium- and high-speed operations. However, low speed instability and instability under various charge perturbation conditions continue to be serious issues in this field of study and have not yet been effectively resolved. Some application such as traction drives and cranes are required to maintain the desired level of torque down to low speed levels with uncertain load torque disturbance conditions. Speed and torque control is more important particularly in motor-in-wheel traction drive train configuration where vehicle wheel rim is directly connected to the motor shaft to control the speed and torque.* ***Novelty*** *of the proposed work is to improve the dynamic performance of conventional controller used of model reference adaptive system speed observer using both type-1 and type-2 fuzzy logic controllers.* ***Purpose.*** *In proposed scheme, the performance of the engine is being controlled, fuzzy logic controller is controlling the estimate rotor speed, and results are then compared using type-1 and type-2.* ***Method****. For a two-wheeled motorized electric vehicle, a high-performance sensorless wheel motor drive based on both type-2 and type-1 fuzzy logic controllers of the model reference adaptive control system is developed.* ***Results.*** *Proved that, using fuzzy logic type-2 controller the sensorless speed control of the electrical differential of electric vehicle EV observer, much better results are achieved.* ***Practical value.*** *The main possibility of realizing reliable and efficient electric propulsion systems based on intelligent observers (type-2 fuzzy logic) is demonstrated. The research methodology has been designed to facilitate the future experimental implementation on a digital signal processor.* References 27, table 3, figures 16.

Key words: **electrical vehicle, induction machines, model reference adaptive system, field oriented control, electric differential, fuzzy logic controller.**

Вступ*. У цій роботі представлений новий підхід до оцінки швидкості колісних електромобілів із двома незалежними задніми приводами. В даний час асинхронний двигун із регульованою швидкістю замінює двигун постійного струму в широкому діапазоні застосувань, включаючи електромобілі, де потрібний швидкий динамічний відгук. Тепер це можливо внаслідок значного покращення динамічних характеристик електроприводів, викликаного технологічними досягненнями та розробками в галузі пристроїв комутації потужності, цифрової обробки сигналів та останнім часом інтелектуальних систем управління. Надійність та стійкість системи підвищуються, а вартість, розмір та вимоги до обслуговування асинхронного двигуна знижуються завдяки стратегіям керування без датчика швидкості. Успішне використання асинхронного двигуна без датчика було виконано для роботи на середніх та високих швидкостях. Проте низькошвидкісна нестабільність і нестабільність за умов збурення заряду продовжують залишатися серйозними проблемами у цій галузі досліджень і досі не вирішені ефективно. У деяких застосуваннях, таких як тягові приводи та крани, потрібно підтримувати бажаний рівень крутного моменту аж до низьких рівнів швидкості з невизначеними умовами збурення крутного моменту навантаження. Контроль швидкості і крутного моменту більш важливий, особливо в конфігурації тягової трансмісії з двигуном в колесі, де обід колеса транспортного засобу безпосередньо з'єднаний з валом двигуна для управління швидкістю і крутним моментом.* ***Новизна*** *запропонованої роботи полягає у поліпшенні динамічних характеристик звичайного регулятора, що використовується в еталонній моделі спостерігача швидкості адаптивної системи з використанням регуляторів нечіткої логіки як першого, так і другого типу.* ***Мета****. У запропонованій схемі контролюються характеристики двигуна, нечіткий логічний контролер управляє оцінною частотою обертання ротора, а потім порівнюються результати з використанням типу 1 і типу 2.* ***Метод****. Для двоколісного моторизованого електромобіля розроблено високопродуктивний бездатчиковий двигун-привід коліс на основі нечітких логічних контролерів як 2-го, так і 1-го типів еталонної системи адаптивного управління.* ***Результати****. Доведено, що з використанням регулятора нечіткої логіки 2-го типу для бездатчикового управління швидкістю EV-спостерігача електричного диференціала електромобіля досягаються значно кращі результати.* ***Практична цінність****. Показано принципову можливість реалізації надійних та ефективних електрореактивних рухових установок на основі інтелектуальних спостерігачів (нечітка логіка 2-го типу). Розроблено методологію дослідження для полегшення майбутньої експериментальної реалізації на цифровому сигнальному процесорі.* Бібл. 27, табл. 3, рис. 16.

Ключові слова: **електромобіль, асинхронні машини, еталонна адаптивна система, полеорієнтоване керування, електричний диференціал, регулятор з нечіткою логікою.**

Introduction. Type-2 fuzzy logic was presented in the mid-70s through the work of Zadeh [1] and later improved by several researchers, with emphasis on the work of Mizumoto and Tanaka [2], and Karnik and Mendel [3]. Type-2 fuzzy logic represents an extension of traditional fuzzy logic (usually called fuzzy logic type-1) or even a second approximation for addressing uncertainties inherent in the real world [4].

Type-2 has been fuzzy logic gaining more and more attention and recognition, especially in systems modeling. While type-1 fuzzy logic presupposes the need for exact knowledge of membership functions, in type-2 fuzzy systems this premise is conceptually questioned, giving rise to so-called type-2 fuzzy sets which, in general terms, offer the possibility of raising the logical and systematic treatment ability for the low accuracy of the information [5]. In this sense, the following very typical situations can be highlighted that suggest the approach or modeling from type-2 fuzzy inference systems:

- identification of fuzzy models for behavior prediction, using noisy data or information;
- rules obtained through information generated by the human expert.

In this sense, type-2 fuzzy logic is effectively applied to the problems of identifying models or inference systems based on human information or that have this as a fundamental element of their construction.

Uncertainties are also present in the daily life of human beings, for example in decision-making, where

uncertain, imprecise, ambiguous or even contradictory terms can be evaluated to originate a decision. Electric vehicles (EVs) are an area where decision-making takes place at all times, in order to promote the movement of the vehicle in a safe, orderly and fast manner. Due to the use of electric motors and inverters in drive systems, electric cars offer many benefits over those powered by internal combustion engines, including quick torque response and independent control of each wheel [6, 7]. Although many control methods with similar benefits have been proposed, their controllers often depend on irrational variables like slip angle and vehicle velocity. Each wheel follows a different trajectory when passing in corners, resulting in a variable distance traveled. This is why differentials are used in automobile technology. The trajectory of the outer wheels also follows a circular arc with a larger radius than that of the inner wheel.

The power transferred to the driving wheels is then divided by the differential, causing the outer wheel to accelerate and the inner wheel to slow down. This suggests that it prevents slippage and improves vehicle handling [8, 9]. There are various benefits when comparing electric differential-based EVs to their conventional counterparts with a central motor. It is undeniable that putting the motors on the wheels substantially simplifies the mechanical design. The electric differential system will minimize the drive line components, improving overall efficiency and dependability [9, 10].

The goal of the paper is the study of Model Reference Adaptive System (MRAS) speed sensorless control is presented where the speed estimation the of in-wheel EVs with 2 independent rear drive was chosen as a case study for the application of a type-2 fuzzy system. Also a comparative study between type-1 and type-2 fuzzy logic controllers (T1FLC, T2FLC) in term of robustness will be simulated and discussed.

Mathematical model of the EV. Dynamics analysis. The vehicle's aerodynamics are taken into account by the control approach suggested in this study, which is not limited to induction motors. This concept is based on the physics and aerodynamics of moving objects. A vehicle's tractive force (F_{te}) is composed of its rolling friction force (F_{rr}), aerodynamic force (F_{ad}), lift force (F_{hc}), acceleration force (F_{la}) and angular acceleration force (F_{wa}):

$$F_{te} = F_{rr} + F_{ad} + F_{hc} + F_{la} + F_{wa}\,. \tag{1}$$

The force that propels the vehicle forward and is transmitted to the ground by the wheels is shown in Fig. 1.

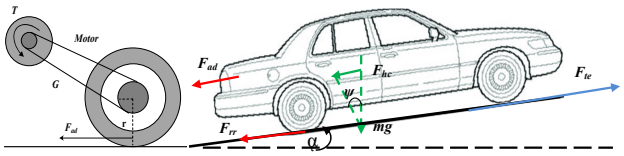

Fig. 1. Elementary forces acting in the EV

The force that will propel the vehicle will depend on the aerodynamic resistance of the vehicles, rolling, auxiliary components and vehicle acceleration if the speed is not constant:

$$F_{rr} = \mu_{rr} \cdot m \cdot g\,, \tag{2}$$

where F_{rr} is the rolling resistive force; μ_{rr} is the rolling resistance coefficient (depends on the tire type and tire pressure, typically on EVs it takes values of 0.005); m is the vehicle mass; g is the gravitational constant.

This resistance depends on the shape of the vehicle, and the way the air surrounds it:

$$F_{ad} = \frac{1}{2} \cdot \rho \cdot A \cdot C_d \cdot \upsilon^2\,, \tag{3}$$

where the aerodynamic force (F_{ad}) characterizes the aerodynamic resistance; ρ is the air density; A is the frontal area of the vehicle; υ is the speed; C_d is the drag coefficient with values typically between 0.3 and 0.19 in a well designed vehicle.

Climb force F_{hc} represents the effort the vehicle makes when climbing a given slope:

$$F_{hc} = m \cdot g \cdot \sin\psi\,, \tag{4}$$

where ψ is the grade angle.

According to Newton's second law, the acceleration force is the force that will apply a linear acceleration to the vehicle:

$$F_{la} = m \cdot a\,, \tag{5}$$

where a is the vehicle acceleration.

For this sizing we need to know what engine torque T is needed to make the wheels rotate:

$$T = \frac{F_{te}}{G} \cdot r\,, \tag{6}$$

where r is the tire radius; F_{te} is the traction force; G is the gear ratio of the engine to the wheel shaft.

The equation in terms of F_{te} is given by:

$$F_{te} = \frac{G}{r} \cdot T\,. \tag{7}$$

The angular speed of the motor will be $\omega = a{\cdot}G/r$, rad·s^{-1}; and the angular acceleration respectively $\dot{\omega} = \upsilon{\cdot}G/r$, rad·s^{-2}; [11, 12].

The torque for this angular acceleration is $T = a{\cdot}J{\cdot}G/r$, where J is the rotor moment of inertia of the motor. The force the wheels need to reach the angular acceleration and determined by:

$$F_{\omega a} = \frac{G}{r} \cdot J \cdot G \cdot \frac{a}{r} = \frac{G^2}{r^2} \cdot J \cdot a\,. \tag{8}$$

Since mechanical systems are not 100 % efficient, we still have to consider the efficiency of the system ρ_g:

$$F_{\omega a} = \frac{G^2}{r^2} \cdot J \cdot a = \frac{G^2}{r^2 \cdot \rho_g} \cdot J \cdot a\,. \tag{9}$$

And finally, the power required to move a vehicle at a speed υ must compensate for the opposing forces:

$$P_{te} = \upsilon F_{te} = \upsilon\left(F_{rr} + F_{ad} + F_{hc} + F_{la} + F_{wa}\right), \tag{10}$$

where υ is the vehicle speed; P_{te} is the vehicle driving power.

Induction motor model and control structure. In this section, the vector technique for induction motor modeling is used, which is important for the study of field oriented control [1, 4]. A system of complex orthogonal axes d and q is defined to represent the three-phase machine. With regard to the flux-current relationship, the dq model can be interpreted as being a two-phase machine with 2 solid and orthogonal magnetic axes d and q [13].

The equations describing the dynamics of the induction motor are:

$$\begin{cases} \bar{u}_s = R_s \bar{i}_s + \sigma L_s \dfrac{\mathrm{d}\bar{i}_s}{\mathrm{d}t} + \dfrac{M}{L_r} \dfrac{\mathrm{d}\bar{\varphi}_s}{\mathrm{d}t} + j\sigma L_s \omega_s \bar{i}_s + j \dfrac{M}{L_r} \omega; \\ 0 = \dfrac{1}{\tau_r} \bar{\varphi}_r - \dfrac{M}{\tau_r} \bar{i}_s + \dfrac{\mathrm{d}\bar{\varphi}_r}{\mathrm{d}t} + j\omega_r \bar{\varphi}_r, \end{cases} \tag{11}$$

where ω_r is the induced rotor current frequency; ω_s is the stator current frequency; j is the inertia; R_s and R_r are the stator and rotor resistances; L_s and L_r are the stator and

rotor inductances; τ_r is the rotor time constant; σ is the leakage flux total coefficient; M is the mutual inductance; ω is mechanical rotor frequency; φ_s and φ_r are the stator and rotor fluxes; i_s and u_s are the rotor current and voltage.

The mechanical equation is written as follows:

$$\Gamma_e - \Gamma_l = j \cdot \frac{\mathrm{d}\Omega}{\mathrm{d}t} + f \cdot \Omega, \quad (12)$$

where Γ_e is the induced electromagnetic torque; Γ_l is the load torque; f is the coefficient of viscous; Ω is the rotor speed.

The electromagnetic torque is:

$$\Gamma_e = \frac{p \cdot M}{L_r}\left(I_{sq} \cdot \varphi_{rd} - I_{sd} \cdot \varphi_{rq}\right), \quad (13)$$

where p is the number of poles pairs.

The observation of stator currents from a fixed reference to a reference flux is what vector modeling in practice aims to achieve. As a result, when a new coordinate system is defined with the direct reference axis, d, or real axis (Re), coincident with the rotor flux vector (φ_r), the component of the rotor flux vector on the quadrature axis, q, or imaginary axis (Im), is eliminated, that is:

$$\varphi_{rq} = 0. \quad (14)$$

The torque determined by (13) can be represented using (14), as follows:

$$T_e = k_c \cdot I_{sq} \cdot \phi_r, \quad (15)$$

where I_{sd} component represents the direct flux; I_{sq} represents the torque control variation, with $k_c = p \cdot M / L_r$.

Speed observer based on MRAS. In the MRAS techniques, rotor speed can be estimated by using 2 estimators (one reference and one adaptive), which estimate the rotor flux components to subsequently use the difference between these estimates to control the speed of the rotor model speed adaptive to the current speed. The MRAS basic setup is shown in (Fig. 2) [14-16].

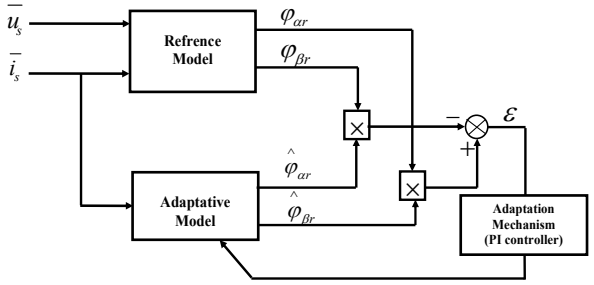

Fig. 2. Induction motor speed estimation using MRAS

The model in the stator reference frame is expressed as:

$$\begin{cases} \bar{u}_s = R_s \cdot \bar{i}_s + \sigma \cdot L_s \cdot \dfrac{\mathrm{d}\bar{i}_s}{\mathrm{d}t} + \dfrac{M}{L_r} \cdot \dfrac{\mathrm{d}\bar{\varphi}_s}{\mathrm{d}t}; \\ 0 = \dfrac{1}{\tau_r} \cdot \bar{\varphi}_r - \dfrac{M}{\tau_r} \cdot \bar{i}_s + \dfrac{\mathrm{d}\bar{\varphi}_r}{\mathrm{d}t} + j \cdot p \cdot \Omega \cdot \bar{\varphi}_r. \end{cases} \quad (16)$$

In the stationary frame (α, β), the time derived from the rotor flux vector is calculated by the MRAS speed observer using 2 independent equations obtained from (4). In [17] are provided these equations which are generally defined as follows:

- the voltage model (reference model):

$$\bar{\varphi}_r = \frac{L_r}{M} \cdot \int \left(\bar{u}_s - R_s \cdot \bar{i}_s\right)\mathrm{d}t - \frac{L_r}{M} \cdot \sigma \cdot L_s \cdot \bar{i}_s; \quad (17)$$

- the current model (adaptive model):

$$\bar{\varphi}_r = \int \left[\left(-\frac{1}{\tau_r} + j \cdot p \cdot \Omega\right)\bar{\varphi}_r + \frac{M}{\tau_r} \cdot \bar{i}_s\right]\mathrm{d}t. \quad (18)$$

Equation (18) can be expressed in an estimated form for the same input:

$$\hat{\bar{\varphi}}_r = \int \left(\frac{M}{\tau_r} \cdot \bar{i}_s - \left(\frac{1}{\tau_r} - j \cdot p \cdot \hat{\Omega}\right)\hat{\bar{\varphi}}_r\right)\mathrm{d}t. \quad (19)$$

The estimation error of the rotor flux is expressed by:

$$\bar{e}_\varphi = \bar{\varphi}_r - \hat{\bar{\varphi}}_r. \quad (20)$$

By subtracting (18) and (19), the dynamic equation of the estimation error is obtained:

$$\dot{\bar{e}}_\varphi = -\left(\frac{1}{\tau_r} - j \cdot p \cdot \Omega\right) \cdot \bar{e}_\varphi + j \cdot p \cdot \left(\Omega - \hat{\Omega}\right) \cdot \hat{\bar{\varphi}}_r. \quad (21)$$

In order to ensure stability of (18); the error ($\bar{\varepsilon}_\phi$) must necessarily this converged to zero [16].

Equation (21) can be rewritten as:

$$\dot{\bar{e}}_k = A \cdot \bar{e}_\varphi - W. \quad (22)$$

To return to ensuring the global stability of the MRAS observer and make the system hyper-stable, we will apply the Lyapunov's stability theorem, where a positive definite function V is chosen such that its derivative is negative semi definite. The proposed function is described in (23). The derivative of this function is shown in (24):

$$V = \bar{e}_\varphi^T \bar{e}_\varphi > 0; \quad (23)$$

$$\dot{V} = \dot{\bar{e}}_\varphi^T \bar{e}_\varphi + \bar{e}_\varphi^T \dot{\bar{e}}_\varphi = \bar{e}_\varphi^T \left(A^T + A\right)\bar{e}_\varphi = -\frac{2}{\tau_r}\bar{e}_\varphi^T \bar{e}_\varphi. \quad (24)$$

The function (24) is negative definite. Inferring the adaptation law from Popov's criterion thus:

$$\int_0^t e_\varphi^T W \mathrm{d}\tau = \int_0^t \left(P \Delta\Omega \begin{bmatrix} e_{\varphi\alpha} & e_{\varphi\beta} \end{bmatrix} J\hat{\bar{\varphi}}_r\right)\mathrm{d}\tau \geq -\delta_o^2. \quad (25)$$

Using the same theorem previously mentioned, assuming that the speed varies slowly, we have:

$$\hat{\Omega} = \delta_0 P \int \begin{bmatrix} e_{\varphi\alpha} & e_{\varphi\beta} \end{bmatrix} J\hat{\bar{\varphi}}_r \mathrm{d}t = \delta_0 P \int \left(e_{\varphi\beta}\hat{\varphi}_{r\alpha} - e_{\phi\alpha}\hat{\varphi}_{r\beta}\right)\mathrm{d}t. \quad (26)$$

There is an incorporated open-loop in the adaption law (offset problem). A low pass filter was recommended in [18] to improve the estimation response.

Equation (26) becomes:

$$\hat{\Omega} = k_p(\bar{\varphi}_r \otimes \hat{\bar{\varphi}}_r) + k_i \int (\bar{\varphi}_r \otimes \hat{\bar{\varphi}}_r)\mathrm{d}t. \quad (27)$$

The classic MRAS observer's poor estimating at low speeds and rotor resistance variation sensitivity is its primary issues. A reviewer provided a number of solutions to this problem. As functional candidates, where an online rotor time constant estimation using the MRAS approach is described in [19-21]. Where the following adaption law gives the estimated value of the inverse rotor time constant ($1/\hat{\tau}_r$):

$$\begin{aligned} 1/\hat{\tau}_r = {} & K_p\left(e_{\phi\alpha}\left(MI_{s\alpha} - \hat{\phi}_{r\alpha}\right) + e_{\phi\beta}\left(MI_{s\beta} - \hat{\phi}_{r\beta}\right)\right) + \\ & + K_i \int \left(e_{\phi\alpha}\left(MI_{s\alpha} - \hat{\phi}_{r\alpha}\right) + e_{\phi\beta}\left(MI_{s\beta} - \hat{\phi}_{r\beta}\right)\right)\mathrm{d}t. \end{aligned} \quad (28)$$

Design of type-2 fuzzy logic controller. The dynamic model of the asynchronous machine is non-linear and strongly coupled, in addition the vehicle dynamics. The use of PI controllers is not suitable for this application; we chose to use fuzzy logic [19-21]. Solutions that are adequate can be found using the T2FLC approach. In this context, we suggest using the T2FLC algorithm to estimate rotor speed in place of the conventional PI of the adaptation mechanism. The rotor flow static and dynamic faults indicated above in (20) serve as the proposed algorithm's inputs and may be expressed as follows [21, 22]:

$$\Delta e_\varphi(k) = e_\varphi(k) - e_\varphi(k-1). \quad (29)$$

The following is how the 3 quantities e_φ, Δe_φ (inputs), $\Delta\hat{\Omega}$ (output) are standardised:

$$e_\varphi = G_{e_\varphi} e_\varphi; \quad \Delta e_\varphi = G_{\Delta e_\varphi} \Delta e_\varphi; \quad \Delta\Omega = G_u \Delta\Omega. \quad (30)$$

The value of the estimated speed is obtained after a discrete integration is performed. Figure 3 shows the structure of the T2FLC created.

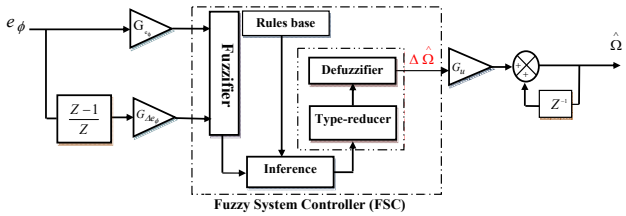

Fig. 3. Proposed type-2 fuzzy logic controllers

The estimated speed constant's expression is as follows:

$$\hat{\Omega}(k) = \hat{\Omega}(k-1) + G_u \Delta\hat{\Omega}(k). \quad (31)$$

The error and variation flux type-2 membership functions are given on the interval [–1, 1] and are similarly determined with Gaussian forms (Fig. 4,*a*). The type-2 fuzzy membership functions of the variation are chosen with intervals form on the interval [–1.5, 1.5] (Fig. 4,*b*).

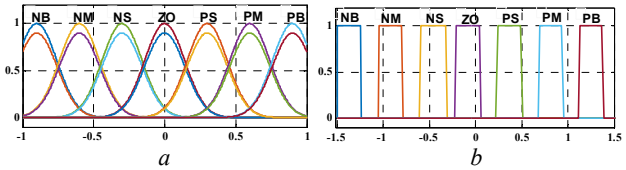

a *b*

Fig. 4. Fuzzy type-2 membership functions to represent: *a* – error and variation flux; *b* – estimated speed

Implementation of the electric differential. Figure 5 shows the implemented system (composed of electrical and mechanical parts) in the MATLAB/Simulink environment.

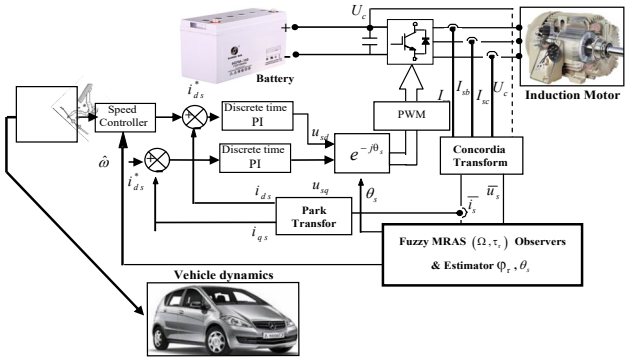

Fig. 5. Basic indirect field oriented control (IFOC) for sensorless IM drives

It should be noted that the 2 inverters share the same DC bus, whose voltage is intended to be steady. In this paper, regenerative braking is not considered. The control system principle could be summarized in 2 principal points:

1) each motor's torque is controlled by a speed network control;

2) speed difference feedback is used to regulate the speed of each rear wheel.

Due to the fact that 2 different motors directly drive the 2 rear wheels, during steering maneuvers, the outer wheel's speed must be higher than the inner wheel's speed (and vice-versa). If the steering wheel's angular speed is sensed by the speed estimator, this condition can be easily met [23-25]. The command for the accelerator pedal then set the common reference speed. The actual reference speeds for the left and right drives are then acquired by modifying the common reference speed using the type-2 fuzzy logic speed estimator's output signal.

The speed of the left wheel of the vehicle rises as it makes a right turn, while the speed of the right wheel stays at the standard reference speed (ω_{ref}). The speed of the right wheel rises when turning to the left, while the speed of the left wheel stays constant at the usual reference speed (ω_{ref}).

The vehicle system model may often be analyzed using a driving trajectory. We used the Ackermann-Jeantaud steering model since it is often used as a driving trajectory. Ackermann steering geometry is a geometric configuration of the steering system's linkages that was created to address the issue of wheels on the inside and outside of bends needing to draw circles with differing radii. Modern vehicles do not employ pure Ackermann-Jeantaud steering, in part because it overlooks significant and compliant effects, although the principle is sound for low-speed maneuvers [26, 27] (Fig. 6).

The following characteristic can be calculated from this model:

$$R = L/\tan\delta, \quad (32)$$

where R is the turn radius; δ is the steering angle; L is the wheel base.

Therefore, the linear speed of each wheel drive is:

$$\begin{cases} V_1 = \omega_v (R - d/2); \\ V_2 = \omega_v (R + d/2), \end{cases} \quad (33)$$

where d is the track width and their angular speed by:

$$\begin{cases} \hat{\omega}_1 = \dfrac{L - (d/2)\tan\delta}{L} \omega_v; \\ \hat{\omega}_2 = \dfrac{L + (d/2)\tan\delta}{L} \omega_v, \end{cases} \quad (34)$$

where ω_v represents the vehicle's angular speed from the turn's center. Therefore, the difference in wheel drive angular speeds is:

$$\Delta\omega = \hat{\omega}_1 - \hat{\omega}_2 = \frac{-d\tan\delta}{L} \omega_v \quad (35)$$

and the direction of the trajectory is indicated by the steering angle:

$$\begin{aligned} &\delta > 0 \Rightarrow \text{turn left;} \\ &\delta = 0 \Rightarrow \text{straight ahead;} \\ &\delta < 0 \Rightarrow \text{turn right.} \end{aligned} \quad (36)$$

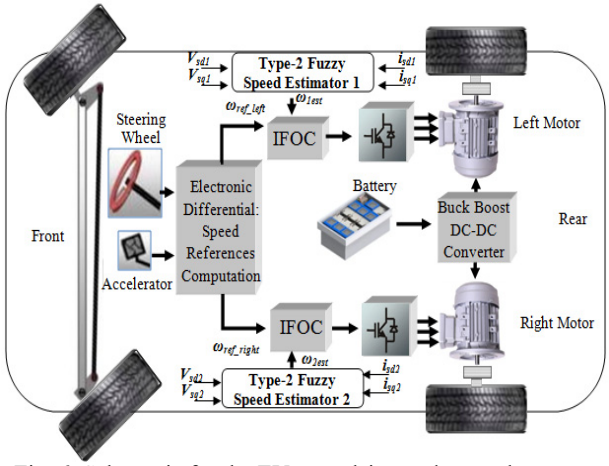

Fig. 6. Schematic for the EV propulsion and control systems

Figure 7 displays the block diagram of the electric differential system employed in simulations that correspond with the equation mentioned above, where $K_1 = 0{,}5$ and $K_2 = -0{,}5$.

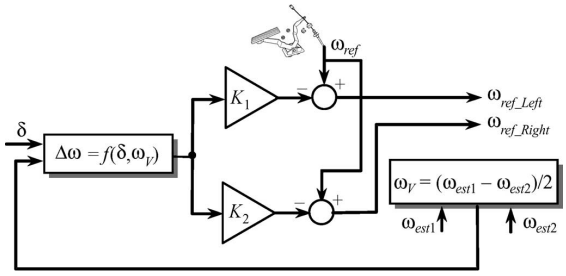

Fig. 7. Block diagram of the electric differential system

The performance of fitness function. The performance of the system is frequently used the IAE (Integral Absolute Error), ITAE (Integral of Time multiplied by Absolute Error), ISE (Integral Squared Error) and ITSE (Integral Time Squared Error) criteria [27]:

$$IAE = \int_0^\infty |e(t)|\mathrm{d}t\,; \tag{37}$$

$$ITAE = \int_0^\infty t|e(t)|\mathrm{d}t\,; \tag{38}$$

$$ISE = \int_0^\infty \{e(t)\}^2\mathrm{d}t\,; \tag{39}$$

$$ITSE = \int_0^\infty t\{e(t)\}^2\mathrm{d}t\,. \tag{40}$$

Simulation and analysis. The test cycle is the urban ECE-15 cycle (Fig. 8). The speed of the vehicle is displayed as a function of time in a driving cycle, which is a collection of data points. It is used to evaluate how well EVs function in urban environments and is distinguished by a modest vehicle speed (50 km/h at most). The first illustration of the electric differential performances is in Fig. 9, which displays the driving speed of each wheel during steering for $0 < t < 1180$ s. The complicated sequence of accelerations, decelerations, and multiple pauses required by the urban ECE-15 cycle clearly demonstrate how well the electric differential functions.

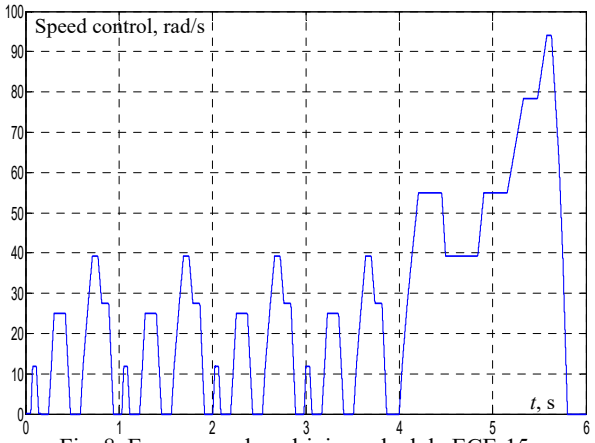

Fig. 8. European urban driving schedule ECE-15

The flux (φ_r) and the developed torque in each wheel drive of the induction motor (left and right) are shown in Fig. 10, 11, respectively, along with variations in the location of the accelerator pedal (Fig. 12) and a variable road profile (rising and descending parts). It should be noted that the variations in flux and torque are as large as variations in the accelerator pedal and the road profile.

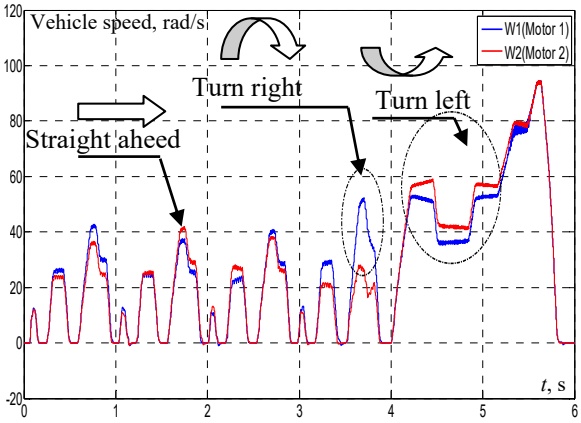

Fig. 9. Vehicle wheels speed

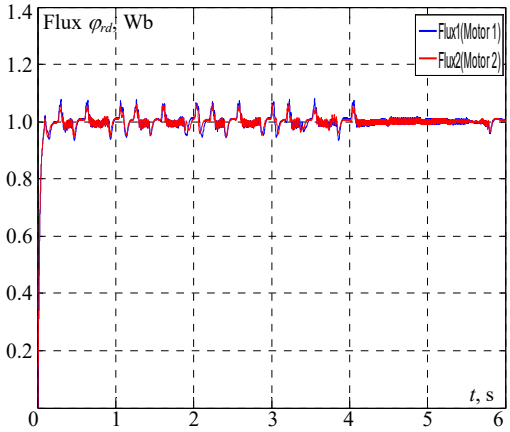

Fig. 10. Flux φ_{rd}

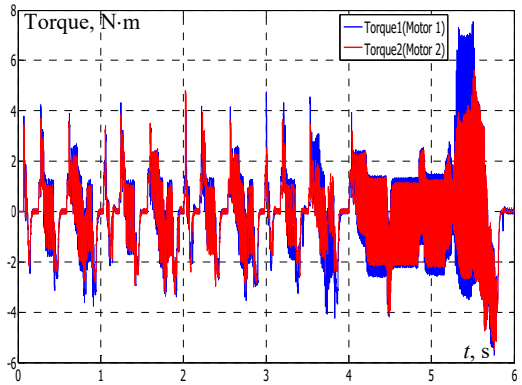

Fig. 11. Torque motors

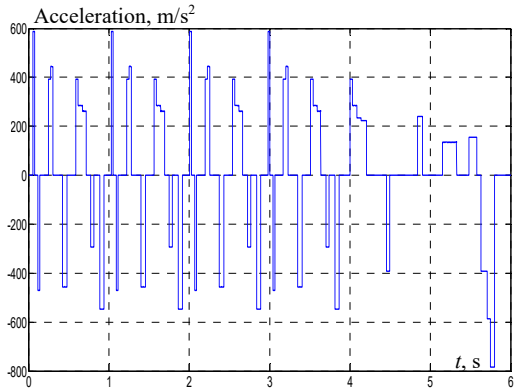

Fig. 12. Acceleration pedal position

Comparative study between T2FLC and T1FLC controllers. A comparison between the simulation results achieved at low-speed zones by T2FLC and T1FLC controllers was done in order to verify the performances of the new control structure employing T2FLC. As illustrated in Fig. 13,*a*, the membership functions of the flux error and its variation are defined on the interval [–1, 1] and are identical in form. In Fig. 13,*b*, the singleton forms over the interval [–2.5, 2.5] are used for the membership functions for the variation in estimated speed.

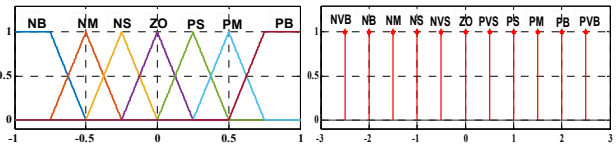

a *b*

Fig. 13. Fuzzy type-1 membership functions to represent: *a* – error and variation flux; *b* – estimated speed

The results provided in Fig. 14 demonstrate the benefit of the suggested observer, the MRAS T2FLC, over the MRAS T1FLC, which shows the measured speed and the estimated value for the different speed as shown in Fig. 15. These figures clearly demonstrate that the estimated speed for this applied profile accurately tracks the measured value even at zero speed. The estimated error between the MRAS T2FLC and MRAS T1FLC is also shown in Fig. 16, and it is immediately apparent that the T2FLC error is significantly smaller than the T1FLC error. It is obvious that the T2FLC controller outperforms its T1FLC predecessor.

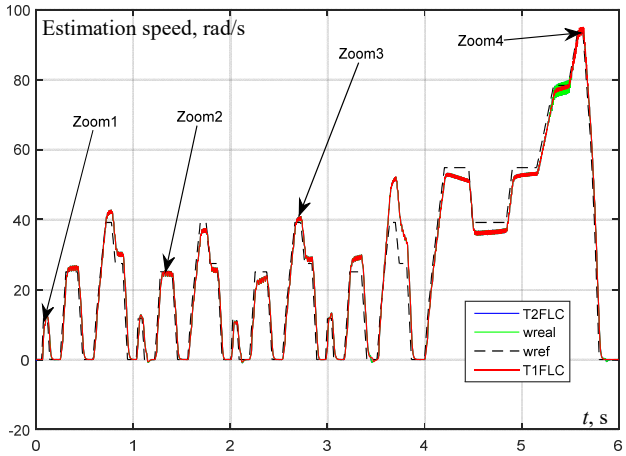

Fig. 14. Estimated and measured vehicle speed

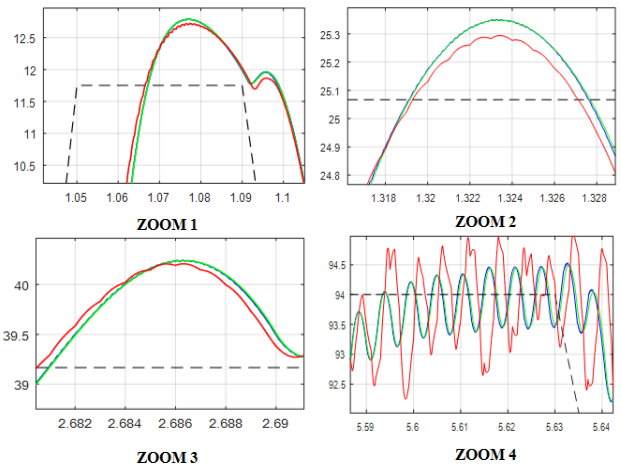

Fig. 15. Zoom of the estimated and measured vehicle speed

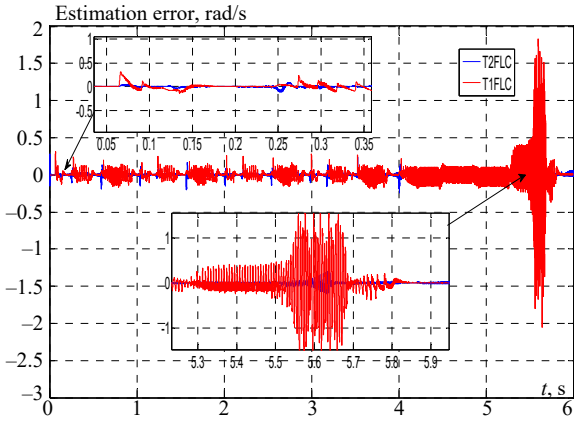

Fig. 16. Speed estimation error

Tables 1, 2 contain comparisons of the results for the various controllers for each of the errors. Our results indicate that the T2FLC technique has better performance than T1FLC controller.

The data of the induction motors are given in Table 3.

Table 1

Performances comparison the first induction motor

Controllers IM1	IAE	ISE	ITAE	ITSE
T1FLC	0.1215	0.0165	0.2995	0.0660
T2FLC	0.0316	0.0014	0.0702	0.0030

Table 2

Performances comparison of the second induction motor

Controllers IM2	IAE	ISE	ITAE	ITSE
T1FLC	0.1160	0.0142	0.2866	0.0552
T2FLC	0.0358	0.0019	0.0846	0.0047

Table 3

Parameters of the induction motor

Rate power P, kW	1.5
Rated stator resistance R_s, Ω	5.72
Rated rotor resistance R_r, Ω	4.2
Rated stator inductance L_s, H	0.462
Rated rotor inductance L_r, H	0.462
Mutual inductance M, H	0.4402
Pole pairs p	2
Inertia J, kg·m^2	0.0049
Friction coefficient f_r, kg·m^2/s	0

Conclusions. In this paper, we introduce a sensorless model reference adaptive system type-2 fuzzy logic controller and observer for electric vehicle electrical differential control. By comparing the results of type-1 and type-2 fuzzy models, it was possible to identify that the type-2 fuzzy model was the best proposal to reproduce the decision making and in the sensorless control of the electrical differential of electric vehicle, especially when driving at high speeds. Also this comparison makes it evident that the model reference adaptive system type-2 fuzzy logic controller approach is effectives. The outstanding performance of the induction motor control is revealed and shown by these data.

Conflict of interest. The authors declare that they have no conflicts of interest.

REFERENCES

1. Zadeh L.A. Fuzzy sets. *Information and Control*, 1965, vol. 8, no. 3, pp. 338-353. doi: https://doi.org/10.1016/S0019-9958(65)90241-X.

2. Mizumoto M., Tanaka K. Some properties of fuzzy sets of type 2. *Information and Control*, 1976, vol. 31, no. 4, pp. 312-340. doi: https://doi.org/10.1016/S0019-9958(76)80011-3.

3. Karnik N.N., Mendel J.M. Applications of type-2 fuzzy logic systems: handling the uncertainty associated with surveys. *FUZZ-IEEE'99. 1999 IEEE International Fuzzy Systems. Conference Proceedings (Cat. No.99CH36315)*, 1999, vol. 3, pp. 1546-1551 doi: https://doi.org/10.1109/FUZZY.1999.790134.
4. Mousavi S.M. A new interval-valued hesitant fuzzy pairwise comparison–compromise solution methodology: an application to cross-docking location planning. *Neural Computing and Applications*, 2019, vol. 31, no. 9, pp. 5159-5173. doi: https://doi.org/10.1007/s00521-018-3355-y.
5. Tsang Y.P., Wong W.C., Huang G.Q., Wu C.H., Kuo Y.H., Choy K.L. A Fuzzy-Based Product Life Cycle Prediction for Sustainable Development in the Electric Vehicle Industry. *Energies*, 2020, vol. 13, no. 15, art. no. 3918. doi: https://doi.org/10.3390/en13153918.
6. Seth A.K., Singh M. Unified adaptive neuro-fuzzy inference system control for OFF board electric vehicle charger. *International Journal of Electrical Power & Energy Systems*, 2021, vol. 130, art. no. 106896. doi: https://doi.org/10.1016/j.ijepes.2021.106896.
7. Williamson S.S., Rathore A.K., Musavi F. Industrial Electronics for Electric Transportation: Current State-of-the-Art and Future Challenges. *IEEE Transactions on Industrial Electronics*, 2015, vol. 62, no. 5, pp. 3021-3032. doi: https://doi.org/10.1109/TIE.2015.2409052.
8. Haddoun A., Benbouzid M.E.H., Diallo D., Abdessemed R., Ghouili J., Srairi K. Modeling, Analysis, and Neural Network Control of an EV Electrical Differential. *IEEE Transactions on Industrial Electronics*, 2008, vol. 55, no. 6, pp. 2286-2294. doi: https://doi.org/10.1109/TIE.2008.918392.
9. Yang J., Zhang T., Zhang H., Hong J., Meng Z. Research on the Starting Acceleration Characteristics of a New Mechanical–Electric–Hydraulic Power Coupling Electric Vehicle. *Energies*, 2020, vol. 13, no. 23, art. no. 6279. doi: https://doi.org/10.3390/en13236279.
10. Tao Guilin, Ma Zhiyun, Zhou Libing, Li Langru. A novel driving and control system for direct-wheel-driven electric vehicle. *2004 12th Symposium on Electromagnetic Launch Technology*, 2004, pp. 514-517. doi: https://doi.org/10.1109/ELT.2004.1398134.
11. Ju-Sang Lee, Young-Jae Ryoo, Young-Cheol Lim, Freere P., Tae-Gon Kim, Seok-Jun Son, Eui-Sun Kim. A neural network model of electric differential system for electric vehicle. *2000 26th Annual Conference of the IEEE Industrial Electronics Society. IECON 2000. 2000 IEEE International Conference on Industrial Electronics, Control and Instrumentation. 21st Century Technologies and Industrial Opportunities (Cat. No.00CH37141)*, vol. 1, pp. 83-88. doi: https://doi.org/10.1109/IECON.2000.973130.
12. Han-Xiong Li, Gatland H.B. A new methodology for designing a fuzzy logic controller. *IEEE Transactions on Systems, Man, and Cybernetics*, 1995, vol. 25, no. 3, pp. 505-512. doi: https://doi.org/10.1109/21.364863.
13. Guezi A., Bendaikha A., Dendouga A. Direct torque control based on second order sliding mode controller for three-level inverter-fed permanent magnet synchronous motor: comparative study. *Electrical Engineering & Electromechanics*, 2022, no. 5, pp. 10-13. doi: https://doi.org/10.20998/2074-272X.2022.5.02.
14. Chekroun S., Abdelhadi B., Benoudjit A. Design optimization of induction motor using hybrid genetic algorithm «a critical analyze». *Advances in Modelling and Analysis C*, 2016, vol. 71, no. 1, pp. 1-23.
15. Naït-Saïd M.-S., Tadjine M., Drid S. Robust backstepping vector control for the doubly fed induction motor. *IET Control Theory & Applications*, 2007, vol. 1, no. 4, pp. 861-868. doi: https://doi.org/10.1049/iet-cta:20060053.
16. Young Ahn Kwon, Dae Won Jin. A novel MRAS based speed sensorless control of induction motor. *IECON'99. Conference Proceedings. 25th Annual Conference of the IEEE Industrial Electronics Society (Cat. No.99CH37029)*, 1999, vol. 2, pp. 933-938. doi: https://doi.org/10.1109/IECON.1999.816537.
17. Khemis A., Benlaloui I., Drid S., Chrifi-Alaoui L., Khamari D., Menacer A. High-efficiency induction motor drives using type-2 fuzzy logic. *The European Physical Journal Plus*, 2018, vol. 133, no. 3, art. no. 86. doi: https://doi.org/10.1140/epjp/i2018-11903-6.
18. Benlaloui I., Drid S., Chrifi-Alaoui L., Ouriagli M. Implementation of a New MRAS Speed Sensorless Vector Control of Induction Machine. *IEEE Transactions on Energy Conversion*, 2015, vol. 30, no. 2, pp. 588-595. https://doi.org/10.1109/TEC.2014.2366473.
19. Zaky M.S., Khater M.M., Shokralla S.S., Yasin H.A. Wide-Speed-Range Estimation With Online Parameter Identification Schemes of Sensorless Induction Motor Drives. *IEEE Transactions on Industrial Electronics*, 2009, vol. 56, no. 5, pp. 1699-1707. doi: https://doi.org/10.1109/TIE.2008.2009519.
20. Vasic V., Vukosavic S. PES News. *IEEE Power Engineering Review*, 2001, vol. 21, no. 11, pp. 16-17. doi: https://doi.org/10.1109/39.961999.
21. Miloud Y., Draou A. Fuzzy logic based rotor resistance estimator of an indirect vector controlled induction motor drive. *IEEE 2002 28th Annual Conference of the Industrial Electronics Society. IECON 02*, vol. 2, pp. 961-966. doi: https://doi.org/10.1109/IECON.2002.1185402.
22. Ali Moussa M., Derrouazin A., Latroch M., Aillerie M. A hybrid renewable energy production system using a smart controller based on fuzzy logic. *Electrical Engineering & Electromechanics*, 2022, no. 3, pp. 46-50. doi: https://doi.org/10.20998/2074-272X.2022.3.07.
23. Bordons C., Ridao M.A., Perez A., Arce A., Marcos D. Model Predictive Control for power management in hybrid fuel cell vehicles. *2010 IEEE Vehicle Power and Propulsion Conference*, 2010, pp. 1-6. doi: https://doi.org/10.1109/VPPC.2010.5729119.
24. Vaez S., John V.I., Rahman M.A. Energy saving vector control strategies for electric vehicle motor drives. *Proceedings of Power Conversion Conference - PCC '97*, vol. 1, pp. 13-18. doi: https://doi.org/10.1109/PCCON.1997.645578.
25. Takeda K., Takahashi C., Arita H., Kusumi N., Amano M., Emori A. Design of hybrid energy storage system using dual batteries for renewable applications. *2014 IEEE PES General Meeting | Conference & Exposition*, 2014, pp. 1-5. doi: https://doi.org/10.1109/PESGM.2014.6938860.
26. Colyer R.E., Economou J.T. Comparison of steering geometries for multi-wheeled vehicles by modelling and simulation. *Proceedings of the 37th IEEE Conference on Decision and Control (Cat. No.98CH36171)*, 1998, vol. 3, pp. 3131-3133. doi: https://doi.org/10.1109/CDC.1998.757992.
27. Xia X., Xing Y., Wei B., Zhang Y., Li X., Deng X., Gui L. A fitness-based multi-role particle swarm optimization. *Swarm and Evolutionary Computation*, 2019, vol. 44, pp. 349-364. doi: https://doi.org/10.1016/j.swevo.2018.04.006.

Received 11.09.2022
Accepted 25.12.2022
Published 01.07.2023

Abderrahmane Khemis[1,2], *Doctor of Technical Science, Associate Professor,*
Tarek Boutabba[1,2], *Doctor of Technical Science, Associate Professor,*
Said Drid [2,3], *PhD, Professor,*
[1] University of Khenchela,
El-Hamma, BP 1252 Road of Batna, Khenchela, 40004, Algeria,
e-mail: khemis05@yahoo.fr; boutabba_tarek@yahoo.fr;
[2] LSPIE Laboratory, University of Batna 2,
53, Constantine road, Fésdis, Batna, 05078, Algeria.
[3] Higher National School of Renewable Energy, Environment and Sustainable Development,
Batna, Constantine road, Fesdis, Batna, 05078, Algeria,
e-mail: s.drid@hns-re2sd.dz (Corresponding Author)

How to cite this article:
Khemis A., Boutabba T., Drid S. Model reference adaptive system speed estimator based on type-1 and type-2 fuzzy logic sensorless control of electrical vehicle with electrical differential. *Electrical Engineering & Electromechanics*, 2023, no. 4, pp. 19-25. doi: https://doi.org/10.20998/2074-272X.2023.4.03